ATMOSPHERIC AND OCEANIC SCIENCE LETTERS, 2011, VOL. 4, NO. 2, 65–69

An Evidence of Aerosol Indirect Effect on Stratus Clouds from the Integrated Ground-Based Measurements at the ARM Shouxian Site

TANG Jin-Ping[1,2], WANG Pu-Cai[1], DUAN Min-Zheng[1], CHEN Hong-Bin[1], XIA Xiang-Ao[1], and LIAO Hong[3]

[1] *Key Laboratory of Middle Atmosphere and Global Environment Observation (LAGEO), Institute of Atmospheric Physics, Chinese Academy of Sciences, Beijing 100029, China*
[2] *Graduate University of Chinese Academy of Sciences, Beijing 100049, China*
[3] *State Key Laboratory of Atmospheric Boundary Layer Physics and Atmospheric Chemistry (LAPC), Institute of Atmospheric Physics, Chinese Academy of Sciences, Beijing 100029, China*

Received 14 October 2010; revised 17 December 2010; accepted 19 December 2010; published 16 March 2011

Abstract The aerosol effect on clouds was explored using remote sensing of aerosol and cloud data at Shouxian, China. Non-precipitation, ice-free, and overcast clouds were firstly chosen by a combination of sky images from the Total Sky Imager (TSI), cloud base heights from the Ceilometer, and vertical temperature profiles from the Balloon-Borne Sounding System (BBSS). Six cases were chosen in summer, and seven in autumn. The averaged cloud effective radii (r_e), cloud optical depth (COD), aerosol total light scattering coefficient (σ), and liquid water path (LWP) are, respectivey, 6.47 μm, 35.4, 595.9 mm^{-1}, 0.19 mm in summer, and 6.07 μm, 96.0, 471.7 mm^{-1}, 0.37 mm in autumn. The correlation coefficient between r_e and σ was found to change from negative to positive value as LWP increases.

Keywords: aerosol, warm cloud, effective radius, optical depth, liquid water path

Citation: Tang, J.-P., P.-C. Wang, M.-Z. Duan, et al., 2011: An evidence of aerosol indirect effect on stratus clouds from the integrated ground-based measurements at the ARM Shouxian site, *Atmos. Oceanic Sci. Lett.*, **4**, 65–69.

1 Introduction

Aerosol affects climate indirectly by changing cloud properties. Higher aerosol loading results in smaller cloud effective radii and larger cloud albedo if the liquid water path (LWP) remains stable, which is called the first aerosol indirect effect (Twomey, 1977). In addition, the decreased cloud-drop effective radius may suppress precipitation and prolong cloud lifetime, which is called the second indirect effect of aerosol (Albrecht, 1989; Ramanathan et al., 2001). In convective clouds, the smaller cloud droplets freeze at higher altitude above cloud base, releasing latent heat higher up in the atmosphere, and potentially invigorating updrafts. This thermodynamic effect may lead to a greater warm cloud greenhouse effect (Devasthale et al., 2005; Koren et al., 2005).

Many observations and modeling efforts have been made to examine the first indirect effect of aerosol on both ice and warm clouds. For ice clouds, Jiang et al. (2008) found suppressed precipitation and reduced cloud effective radius associated with polluted ice clouds during the dry season in South America, when the aerosol optical depth observed by Moderate Resolution Imaging Spectroradiometer (MODIS) is highly correlated with carbon monoxide (CO) concentrations observed by the Microwave Limb Sounder (MLS) on the Aura Satellite. Alternatively, Chylek et al. (2006) analyzed MODIS data and found that ice particles in clouds over the Indian Ocean shifted towards larger size with increased regional pollution during winter. Using the same dataset, Massie et al. (2007) concluded that the size of liquid droplets decreased with an increase in aerosol optical depth while ice particles exhibited little change in size. The controversial results obtained by Chylek et al. (2006) and Massie et al. (2007) are likely associated with differences in updraft velocity because the number of ice particles that are nucleated is proportional to the updraft velocity (Kärcher and Lohmann, 2003).

Min and Harrison (1996) proposed an algorithm to retrieve warm cloud optical properties from the ground-based solar spectral measurements. Using this algorithm, Kim et al. (2003) and Feingold et al. (2003) have showed weak negative correlation between warm cloud effective radii and aerosol light scattering coefficients at the U.S. Southern Great Plains in 2000. The negative correlation was observed by satellites in South America (Menon and Rotstayn, 2006) and over the ocean (Nakajima et al., 2001; Kaufman et al., 2005). However, some positive correlations were presented along the coasts of South China and Mexico (Yuan et al., 2008). The uncertainties in the correlation between aerosol loading and warm cloud properties may result from uncertainties in geographical conditions, time periods, and other influential factors such as cloud and aerosol vertical profile (Costantino and Bréon, 2010), aerosol chemical composition (Han et al., 1994), aerosol size distribution (Rosenfeld et al., 2008), cloud geometric thickness (Pandithurai et al., 2009), vertical wind shear (Kim et al., 2003), convergence (Mauger and Norris, 2007), and adiabaticity (Kim et al., 2008).

Several investigations on aerosol indirect effects The experiments at the SGP are still doing, so I should use the form conducted in South America and the Southern Great Plains. However, the aerosol indirect effects may show unique characteristics in China, especially in Southeast

Corresponding author: TANG Jin-Ping, Tangjp@mail.iap.ac.cn

China, where the East Asian Monsoon dominates and emissions from anthropogenic (e.g., sulfate, nitrate, soot) and natural (e.g., dust) sources form heavy aerosol loading (Qiu, 2009). To monitor this area of China, Atmospheric Radiation Measurement (ARM) mobile facilities were installed at Shouxian, Anhui Province, from May to December 2008. In this paper, we investigate aerosol effects on cloud properties such as optical depth and effective radius using the integrated measurement data.

2 The Aerosol and cloud data and methodology

ARM facilities were deployed during May to December 2008, at Shouxian, China (32.56°N, 116.78°E, 22.7 meters above the sea level). One of major the objective is to study the aerosol-cloud interactions. The measurements of surface irradiances, LWP, the light scattering coefficient of aerosols, and cloud base height were carried out in the campaign. The spectral total-horizontal, diffuse-horizontal, and direct-normal irradiances were measured every 20 seconds at wavelengths of 415, 500, 610, 665, 862, and 940 nm by a Multi-Filter Rotating Shadowband Radiometer (MFRSR). The total LWP was also measured every 20 s by a microwave radiometer (MWR), a passive instrument that measures column integrated water vapor and liquid water based on microwave emissions of atmospheric water vapor and liquid water molecules at 23.8 GHz and 31.4 GHz. Typical uncertainties in the column integrated liquid water are 0.02 mm (20 g m^{-2}) (Pandithurai et al., 2009). The aerosol total light scattering coefficients (σ) were measured by the nephelometer (Model 3563) at 450, 550, and 700 nm in the Aerosol Observing System. Because σ at three wavelengths varies little with time, we used the σ at 450 nm here, however, the 450-nm σ value is also the largest. Lastly, the cloud base height were collected by the Ceilometer.

The first aerosol indirect effect estimate is based on changes in cloud effective radius (r_e) and cloud optical depth (COD) for change in aerosol loading. We substituted σ for cloud condensation nuclei (CCN), since the correlation between σ and CCN is as high as 0.98 (Pandithurai et al., 2009). Using a nonlinear retrieval based on an adjoint method of radiative transfer developed by Min and Harrison (1996), the r_e and COD were retrieved from irradiance data measured by MFRSR and LWP data measured by MWR. Appling to non-precipitate, ice-free, and overcast clouds, this method first calculated atmospheric transmittance as the ratio of the surface total-horizontal irradiances at 415 nm to the irradiance at the top of the atmosphere (TOA). Langley regression of the direct-normal irradiance taken on clear stable days was used to extrapolate the instrument's response to the TOA (Min and Harrison, 1996; Harrison and Michalsky, 1994), and was then applied to the total-horizontal irradiance. The surface albedo can be obtained from the direct-to-diffuse irradiance ratios available from the MFRSR on cloud-free days. Then the COD is obtained using the calculated atmospheric transmittance and surface albedo by a Nonlinear Least Squares Method. The r_e is retrieved by atmospheric transmittance and LWP based on an adjoint method (Min et al., 2003; Duan and Min, 2005). The evaluation against the airborne in situ measurements showed that the retrieved r_e agreed well with the observations within an error of 5.5% (Min et al., 2003).

To separate the non-precipitation, ice-free, and overcast clouds from others, we carried out a combined analysis of sky images observed every minute by the Total Sky Imager (TSI), cloud base heights measured every 15 s by Ceilometer, and vertical temperature profiles four times a day by the Balloon-Borne Sounding System (BBSS). First, the overcast, non-precipitation clouds were selected by checking the sky images recorded by TSI. Second, the droplet phases of the selected cloud were estimated to distinguish warm (liquid) cloud further from all other clouds. In previous studies, the cloud droplet phase was determined by cloud radar or cloud top temperature from satellite (Feingold et al., 2003), however we estimated the cloud droplet phases with observed cloud base height and temperature profiles observed by BBSS. Observations indicate that the average geometric height of cloud is about 0.9–2 km (Li et al., 2009), and as a result, we designated warm clouds by cloud base heights at least 2 km lower than 0°C atmosphere layer. With these two criteria, we selected six days in summer and seven days in autumn for investigation in this study, obtaining an average distance between measured cloud base and 0°C atmosphere layer of 3.5 km.

3 Results

3.1 Case study

Using a five minute average across all parameters, Fig. 1 shows the measured cloud base heights (Fig. 1a), the retrieved COD and the measured LWP (Fig. 1b), the retrieved r_e (Fig. 1c), and the measured σ (Fig. 1d) on 27 June 2008. The cloud base height is approximately 500 m (Fig. 1a). The balloon measurements show that cloud base height 3.5 km lower than the 0°C atmosphere layer and indicate observed clouds primarily composed of water droplets rather than ice nuclei. The sky images from TSI also support this judgment by showing non-precipitation, overcast cloud throughout the day.

As seen in Fig. 1b, the COD and LWP yield a positive correlation coefficient of 0.58 (at 99.9% significance level), close to the estimate of 0.63 in Kim et al. (2003). This is also supported by the empirical relation proposed by Hansen and Travis (1974):

$$\tau = \int_{z=0}^{h} \frac{3q_L}{2\rho_w r_e} \mathrm{d}z, \tag{1}$$

where ρ_w is the density of liquid water, h is cloud thickness, τ is the COD, which is dependent on the liquid water content q_L (g m^{-3}) and r_e (μm), and q_L is associated with LWP (g m^{-2}, 1 kg m^{-2} = 1 mm) by

$$\mathrm{LWP} = \int_{z=0}^{h} q_L \mathrm{d}z\,. \tag{2}$$

The r_e also affects COD, especially when LWP is

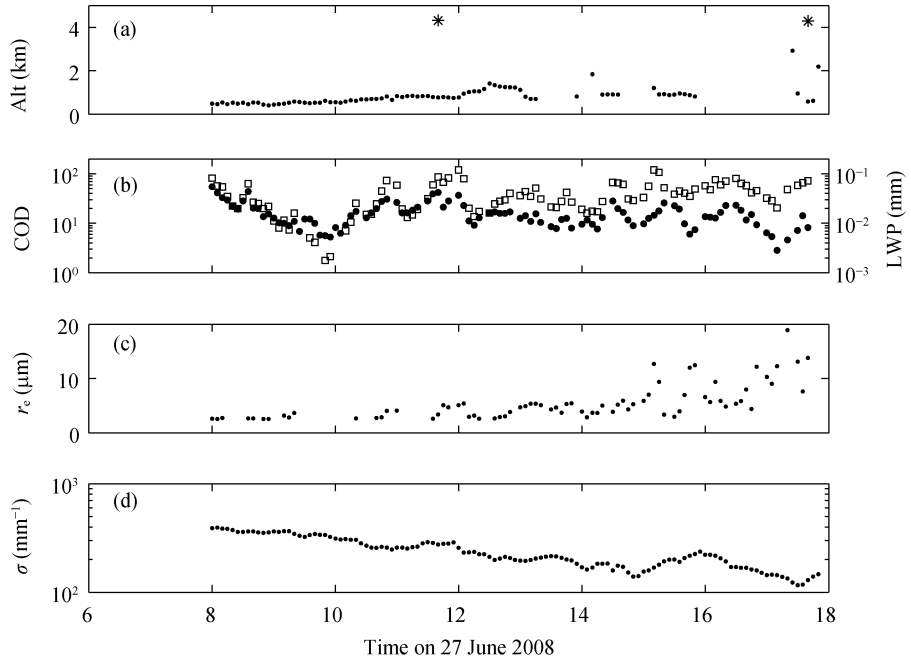

Figure 1 (a) Cloud base altitude (Alt) measured by the Ceilometer at ground level (dotted line) and the altitude at which the temperature are 4°C measured by balloon (asterisks); (b) the retrieved COD (squares) and the liquid water path (LWP, dotted line); (c) the retrieved cloud effective radius; and (d) the observed aerosol extinction coefficient.

nearly constant according to Eq. (1). The LWP for the chosen case was about 0.01–0.12 mm from 1030 to 1740 LST. During this time period, the variation of COD was negatively correlated with that of r_e (Fig. 1c), and the correlation coefficient was –0.47 (at 99.9% significance level). This relationship remains consistent with Eq. (1) and indicates that the increase in cloud effective radii may decrease the scattering capability of cloud droplets and lead to a reduction in COD.

Increased r_e (Fig. 1c) may be explained by the decrease in aerosol concentration proportional to the σ in Fig. 1d. When the LWP is nearly constant, the higher density of aerosol particles, the more available cloud nucleus competing for limited water supply, leading to an increase in the number of cloud droplets while a decrease in the cloud effective radii (Twomey, 1977). The calculated correlation coefficient between σ and r_e is –0.49 (at 99.9% significance level). Additionally, Feingold et al. (2003) quantified the aerosol indirect effect by IE, which is defined as the negative of the slope of log r_e over log σ:

$$\mathrm{IE} = -\mathrm{d}\ \log\ r_e/\mathrm{d}\ \log\sigma. \qquad (3)$$

For homogeneous clouds and constant LWP, a typical value for IE is between 0 and 0.33 (Feingold et al., 2003); an IE of zero may suggest no influence of aerosol loading on r_e, whereas a value of 0.33 would indicate linear proportionality between aerosol number concentration and cloud droplet number concentration. For the data set from 1030 to 1740 LST on 27 June 2008, we obtained an IE of 0.32.

3.2 Dependence of the relation between aerosol and cloud on the LWP

Six and seven cases of non-precipitation warm clouds were selected in summer (days between July and August) and in autumn (days between September and October), respectively. Summer average values for r_e, COD, σ, and LWP were 6.47 μm, 35.4, 595.9 mm^{-1}, and 0.19 mm, and autumn average values were 6.07 μm, 96.0, 471.7 mm^{-1}, and 0.37 mm. Possibly due to more frequent precipitation, LWP in summer is smaller than in autumn. We investigated the first indirect effect of aerosol on warm cloud using the correlation between r_e and σ. As Fig. 2 shows, when LWP is between 0–0.2 mm and 0.35–0.55, the correlation coefficients between r_e and σ are –0.5 and 0.6, respectively. To further examine the dependence of the relation between r_e and σ on the LWP, we divided the total LWP in a range of 15 subintervals from 0 to 0.9 mm with widths of 0.2 mm and midpoint values increasing from 0.1 to 0.8 mm with 0.05 mm steps. Within each subinterval, we calculate the correlation coefficient between r_e and σ (Fig. 3). In summer (Fig. 3a) and autumn (Fig. 3b), the correlation coefficients between r_e and σ vary from negative to positive as LWP increases. When average LWP of subinterval is lower than 0.2 mm, the σ is negatively correlated with r_e, indicating that aerosol particles compete for limited water content and the cloud water droplet can not increase to a large size if the particle number is high. Alternatively, when LWP is higher than 0.2 mm, the correlation becomes positive, indicating that enough water supply and frequent collision or coalescence may help increase the size of cloud droplets if the aerosol particles are abundant. Although the number of samples within some intervals in summer is smaller than 40, as seen in the blue points in Fig. 3a, the changing correlations between r_e and σ along with LWP show similar tendency as that in autumn (Fig. 3b). This interesting phenomenon

reveals the complexity of aerosol indirect effects.

3.3 Distributions of cloud and aerosol properties

As described in 3.1 and 3.2, the cloud properties are influenced by aerosol loading and LWP. To further verify the result, we analyzed the distributions of the cloud and aerosol properties. The total ranges of values of r_e, COD, σ, and LWP in different seasons are divided into 20 bins, the average value at each bin is shown in Fig. 4. The bars in Figs. 4a–d show the distributions of the r_e, COD, σ, and LWP respectively, in summer, with Figs. 4e–h displaying autumn results. All four parameters show peak probability density (PPD): r_e, COD, σ, and LWP appear at 2.67 μm, 14, 961.7 mm^{-1}, and 0.03 mm in summer and at 4.04 μm, 113.88, 189.7 mm^{-1}, and 0.49 mm in autumn. The PPD of COD and r_e in autumn is much larger than in summer, a possible attribute of the large PPD of LWP and small PPD of σ in autumn.

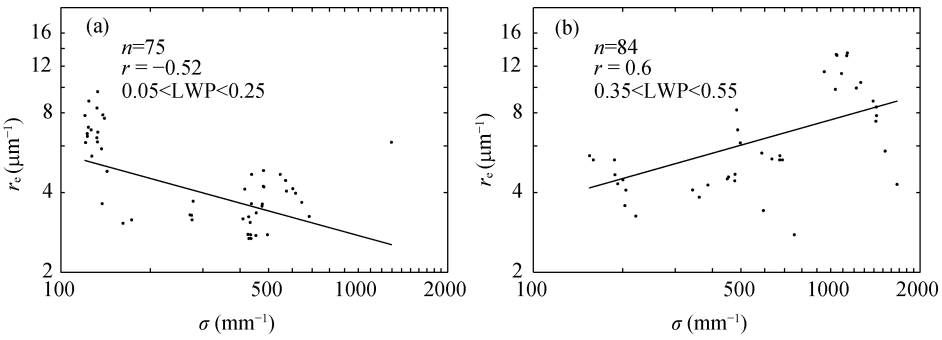

Figure 2 The correlation between σ and r_e in autumn when the LWP is around 0.05–0.25 and 0.35–0.55 in Figs. 2a and 2b, respectively. In the figure, n is the number of data, r is the correlation coefficient between σ and r_e.

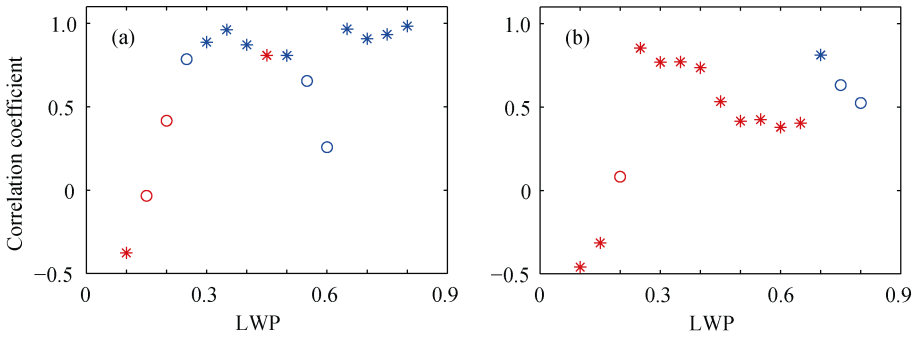

Figure 3 Correlation coefficients between r_e and σ at different LWP subintervals in (a) summer and (b) autumn. Points indicate that the correlation coefficients pass the 95% significance test, while asterisks indicate that they do not pass. The blue dots and stars show that the number in each interval is less than 40, while the red dots show those greater than 40.

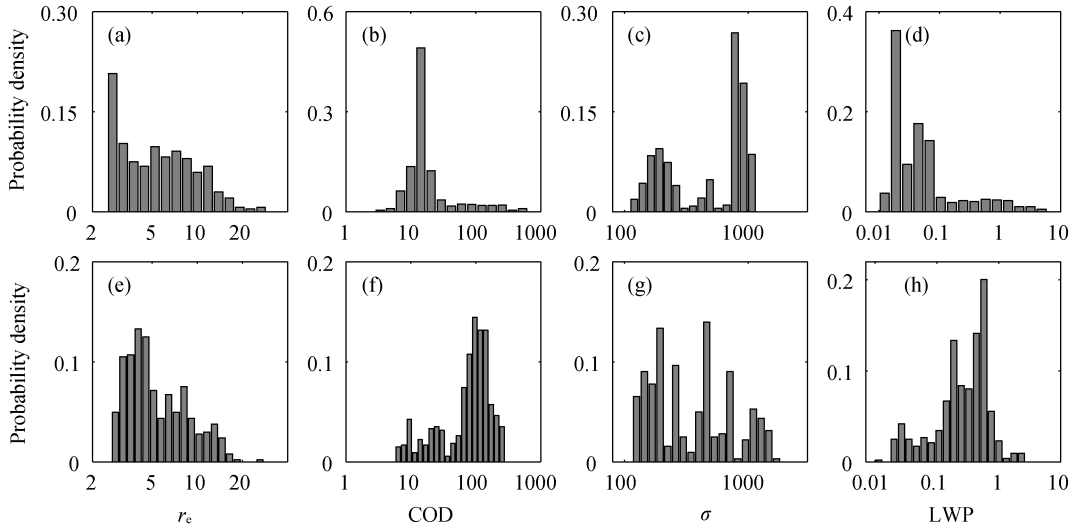

Figure 4 The distribution of (a) r_e (μm), (b) COD, (c) σ (mm^{-1}), and (d) LWP (mm) in summer. (e)–(h) are the same as (a)–(d) but for the cases in autumn.

4 Conclusions and discussion

This study presents the analysis of aerosol first indirect effect in terms of correlation between aerosol and cloud effective radius and cloud optical depth in non-precipitation, ice-free, and overcast clouds. The result shows that both the dependence of the r_e and COD on aerosol loading may be influenced by the magnitude of LWP. The correlation coefficient between r_e and σ varies from negative to positive value as LWP increases.

Our results may be influenced by following factors not considered in this paper. First, the aerosol extinction coefficient we used here was obtained on the ground level and it may be different from the value at the base of cloud layer. Secondly, the cloud macro and micro properties are more or less dependent on atmospheric dynamics (Kaufman et al., 2005; Mauger and Norris, 2007), which is not ruled out in this work. Finally, the aerosol indirect effect may also be affected by the vertical profile of the aerosol, the types of aerosol, and the aerosol chemical composition (Han et al., 1994). As a result, additional comprehensive investigations are needed to understand the aerosol-cloud interaction.

Acknowledgements. This research was supported by the Knowledge Innovation Program of the Chinese Academy of Sciences (KZCX2-YW-QN201), the National Basic Research Program of China (973 Program) (2006CB403706 and 2010CB950804), and the National Natural Science Foundation of China (40775009 and 40875084).

References

Albrecht, B., 1989: Aerosols, cloud microphysics, and fractional cloudiness, *Science*, **245**(4923), 1227, doi:10.1126/science.245.4923.1227.

Chylek, P., M. K. Dubey, U. Lohmann, et al., 2006: Aerosol indirect effect over the Indian Ocean, *Geophys. Res. Lett.*, **33**(6), L06806, doi:10.1029/2005gl025397.

Costantino, L., and F.-M. Bréon, 2010: Analysis of aerosol-cloud interaction from multi-sensor satellite observations, *Geophys. Res. Lett.*, **37**(11), L11801, doi:10.1029/2009GL041828.

Devasthale, A., O. Kruger, and H. Grassl, 2005: Change in cloud-top temperatures over Europe, *IEEE Geosci. Remote Sens. Lett.*, **2**(3), 333–336, doi:10.1109/lgrs.2005.851736.

Duan, M., and Q. Min, 2005: A semi-analytic technique to speed up successive order of scattering model for optically thick media, *JQSRT*, **95**, 21–32, doi:10.1016/j.jqsrt.2004.09.027.

Feingold, G., W. Eberhard, D. Veron, et al., 2003: First measurements of the Twomey indirect effect using ground-based remote sensors, *Geophys. Res. Lett.*, **30**(6), 1287, doi:10.1029/2002GL016633.

Han, Q. Y., W. B. Rossow, and A. A. Lacis, 1994: Near-global survey of effective droplet radii in liquid water clouds using ISCCP data, *J. Climate*, **7**(4), 465–497, doi:10.1175/1520-0442(1994)007<0465:NGSOED>2.0.CO;2.

Hansen, J., and L. Travis, 1974: Light scattering in planetary atmospheres, *Space Sci. Rev.*, **16**(4), 527–610.

Harrison, L., and J. Michalsky, 1994: Objective algorithms for the retrieval of optical depths from ground-based measurements, *Appl. Opt.*, **33**(22), 5126–5132, doi:10.1364/AO.33.005126.

Jiang, J. H., H. Su, M. Schoeberl, et al., 2008: Clean and polluted clouds: Relationships among pollution, ice clouds, and precipitation in South America, *Geophys. Res. Lett.*, **35**, L14804, doi:10.1029/2008GL034631.

Kärcher, B., and U. Lohmann, 2003: A parameterization of cirrus cloud formation: Heterogeneous freezing, *J. Geophys. Res.*, **108**, 4402, doi:10.1029/2002JD003220.

Kaufman, Y. J., I. Koren, L. A. Remer, et al., 2005: The effect of smoke, dust, and pollution aerosol on shallow cloud development over the Atlantic Ocean, *Proc. Nat. Acad. Sci. USA*, **102**(32), 11207–11212, doi:10.1073/pnas.0505191102

Kim, B., M. Miller, S. Schwartz, et al., 2008: The role of adiabaticity in the aerosol first indirect effect, *J. Geophys. Res.*, **113**(5), doi:10.1029/2007JD008961.

Kim, B., S. Schwartz, M. Miller, et al., 2003: Effective radius of cloud droplets by ground-based remote sensing: Relationship to aerosol, *J. Geophys. Res.*, **108**, 4740, doi:10.1029/2003JD003721.

Koren, I., Y. J. Kaufman, D. Rosenfeld, et al., 2005: Aerosol invigoration and restructuring of Atlantic convective clouds, *Geophys. Res. Lett.*, **32**(14), doi:10.1029/2005gl023187.

Li, J., J. Huang, Y. Yi, et al., 2009: Analysis of vertical distribution of cloud in east Asia by space-based lidar data, *Chinese J. Atmos. Sci.* (in Chinese), **33**(4), 698–707.

Massie, S. T., A. Heymsfield, C. Schmitt, et al., 2007: Aerosol indirect effects as a function of cloud top pressure, *J. Geophys. Res.*, **112**(D6), doi:10.1029/2006JD007383.

Mauger, G. S., and J. R. Norris, 2007: Meteorological bias in satellite estimates of aerosol-cloud relationships, *Geophys. Res. Lett.*, **34**(16), doi:10.1029/2007GL029952.

Menon, S., and L. Rotstayn, 2006: The radiative influence of aerosol effects on liquid-phase cumulus and stratiform clouds based on sensitivity studies with two climate models, *Climate Dyn.*, **27**(4), 345–356, doi:10.1007/s00382-006-0139-3.

Min, Q., M. Duan, and R. Marchand, 2003: Validation of surface retrieved cloud optical properties with in situ measurements at the Atmospheric Radiation Measurement Program (ARM) South Great Plains site, *J. Geophys. Res.*, **108**(D17), 4547, doi:10.1029/2003JD003385.

Min, Q., and L. C. Harrison, 1996: Cloud properties derived from surface MFRSR measurements and comparison with GOES results at the ARM SGP site, *Geophys. Res. Lett.*, **23**(13), 1641–1644, doi:10.1029/96GL01488.

Nakajima, T., A. Higurashi, K. Kawamoto, et al., 2001: A possible correlation between satellite-derived cloud and aerosol microphysical parameters, *Geophys. Res. Lett.*, **28**(7), 1171–1174, doi:10.1029/2000GL012186.

Pandithurai, G., T. Takamura, J. Yamaguchi, et al., 2009: Aerosol effect on cloud droplet size as monitored from surface-based remote sensing over East China Sea region, *Geophys. Res. Lett.*, **36**, doi:10.1029/2009GL038451.

Qiu, J., 2009: Atmospheric science: Cloudy, with a chance of science, *Nature*, **461**, 466–468.

Ramanathan, V., P. J. Crutzen, J. T. Kiehl, et al., 2001: Aerosols, climate, and the hydrological cycle, *Science*, **294**(5549), 2119–2124, doi:10.1126/science.1064034.

Rosenfeld, D., U. Lohmann, G. B. Raga, et al., 2008: Flood or drought: How do aerosols affect precipitation? *Science*, **321**(5894), 1309–1313.

Twomey, S., 1977: The influence of pollution on the shortwave albedo of clouds, *J. Atmos. Sci.*, **34**(7), 1149–1152.

Yuan, T. L., Z. Q. Li, R. Y. Zhang, et al., 2008: Increase of cloud droplet size with aerosol optical depth: An observation and modeling study, *J. Geophys. Res.*, **113**(D4), doi:10.1029/2007jd008632.